Earth Syst. Dynam. Discuss., 2, 241–270, 2011
www.earth-syst-dynam-discuss.net/2/241/2011/
doi:10.5194/esdd-2-241-2011

Earth System Dynamics Discussions

Climate change, in the framework of the constructal law

M. Clausse[1], F. Meunier[1], A. H. Reis[2], and A. Bejan[3]

[1]Laboratory of Chemical Engineering applied to Environment, Energy and Health (LGP2ES-EA21), Conservatoire National des Art et Metiers (CNAM), case 331, 292, rue St Martin, 75141 Paris Cedex 03, France
[2]Department of Physics and Evora Geophysics Centre, University of Évora, Ramalho, 59, 7000-67 1 Evora, Portugal
[3]Department of Mechanical Engineering, Duke University, Durham, NC 27708-0300, USA

Received: 21 December 2010 – Accepted: 7 February 2011 – Published: 7 March 2011

Correspondence to: A. H. Reis (ahr@uevora.pt)

Published by Copernicus Publications on behalf of the European Geosciences Union.

Abstract

Here we present a simple and transparent alternative to the complex models of Earth thermal behavior under time-changing conditions. We show the one-to-one relationship between changes in atmospheric properties and time-dependent changes in temperature and its distribution on Earth. The model accounts for convection and radiation, thermal inertia and changes in albedo (ρ) and greenhouse factor (γ). The constructal law is used as the principle that governs the evolution of flow configuration in time, and provides closure for the equations that describe the model. In the first part of the paper, the predictions are tested against the current thermal state of Earth. Next, the model showed that for two time-dependent scenarios, ($\delta\rho = 0.002$; $\delta\gamma = 0.011$) and ($\delta\rho = 0.002$; $\delta\gamma = 0.005$) the predicted equatorial and polar temperature increases and the time scales are ($\Delta T_H = 1.16$ K; $\Delta T_L = 1.11$ K; 104 years) and (0.41 K; 0.41 K; 57 years), respectively. In the second part, a continuous model of temperature variation was used to predict the thermal response of the Earth's surface for changes bounded by $\delta\rho = \delta\gamma$ and $\delta\rho = -\delta\gamma$. The results show that the global warming amplitudes and time scales are consistent with those obtained for $\delta\rho = 0.002$ and $\delta\gamma = 0.005$. The poleward heat current reaches its maximum in the vicinity of 35° latitude, accounting for the position of the Ferrel cell between the Hadley and Polar Cells.

1 Introduction

In this paper we present in simple terms the relationship between changes in average atmospheric properties and time-dependent changes in the distribution of temperature on Earth. We focus on the predictable relationship between these two phenomena, not on what may cause changes in the atmosphere. We show that if the atmospheric changes are known or predicted, climate response is predictable in concise and transparent terms.

ESDD
2, 241–270, 2011

Two recent articles (Bejan and Reis, 2005; Reis and Bejan, 2006) showed how to use the constructal law to predict the essential features of global climate and atmospheric and oceanic circulation. This was demonstrated in simple and direct terms (with pencil and paper) by combining the constructal law with a simple model of the Earth as a heat engine connected to a brake, i.e. an engine with zero delivery of mechanical power to an external user. In accordance with the constructal law, the access of the convective heat current flowing from the warm zone of the Earth to the cold zones was maximized. This was achieved by properly sizing the areas of the warm and cold zones, i.e. by generating the configuration (the design) of the flow system, and from this resulted the basic climate features, which match observations.

The work described in Bejan and Reis (2005) and Reis and Bejan (2006) was based on steady-state and quasisteady (periodic, diurnal) models. Its success recommends its application to elucidating what is perhaps the biggest issue in geophysics today: climate change, its time scale, and how to make its treatment and understanding accessible with pencil and paper, or chalk on the blackboard. In this article we unveil the relationship between changes in the radiative properties of the atmosphere (albedo, greenhouse factor) and time-dependent changes in the global climate. Key features of this relationship are the time scale and magnitude of the changes.

Before plunging into details, we draw attention to the two significant bodies of literature to which this new work belongs. First, the constructal law has been applied with success to predict pattern in nature in many domains other than global climate, for example, river basins scaling, the distribution of human settlements in geography, animal locomotion (running, flying, swimming, sports evolution), dendritic solidification, turbulent flow structure, human dynamics (e.g. urban design, city traffic), allometric scaling in biology, cracks in shrinking solids, dendritic aggregation of dust particles, heterogeneous multiscale porous media, etc. This literature was reviewed in Bejan (1997, 2000, 2006), Reis (2006) and Bejan and Lorente (2006).

Second, in geophysics there is a significant body of work based on ad-hoc invocations of optimality, for example, maximum entropy production (MEP) in Malkus (1954),

ESDD
2, 241–270, 2011

Climate change, in the framework of the constructal law

M. Clausse et al.

Lorenz (1955), Paltridge (1975, 1978), Schulman (1977), North (1981), Lin (1982), Swenson (1989) and Lorenz et al. (2001). This work was reviewed in Reis and Bejan (2006) and Whitfield (2006) and is not reviewed again here. It suffices to say that the constructal law is different than MEP because the constructal law is a general statement of physics, about a physics *phenomenon* that had been overlooked: the time evolution (generation) of flow configuration (design). It is not about the end result (max, min, or optimal), but about the time direction of the phenomenon itself. It applies across the board, from geophysics to biology, engineering and social dynamics.

The constructal law was proposed as a self-standing law of physics in 1996: "For a finite-size flow system to persist in time (to live), its configuration must change in such a way that it provides easier and easier access to the currents that flow through it" (Bejan, 1997). The direction of the "movie tape" of flow configuration evolution is the law: existing flow configurations are being replaced in time by easier flowing configurations.

2 Model

We use the model proposed in Reis and Bejan (2006); (see Fig. 1). The surface temperature is quasi-steady: it is averaged over many daily cycles and annual cycles, but it changes slowly with the changes in the radiative properties of the atmosphere. The surface is not isothermal: it is divided into an equatorial zone of area A_H and temperature $T_H(t)$, and a polar zone of total area A_L and temperature $T_L(t)$. The total surface is fixed

$$A_H + A_L = A = 4\pi R^2 \quad (1)$$

where R is the Earth radius. In the following analysis we use the dimensionless area fraction x, which is defined as

$$x = A_H/A \qquad (1-x) = A_L/A \quad (2)$$

The thermal inertia of the Earth's crust is modeled as a layer of ocean water of average depth h (equal to 2750 m), which covers the entire globe. This h value is obtained

ESDD
2, 241–270, 2011
Climate change, in the framework of the constructal law
M. Clausse et al.

by taking the total volume of ocean water and dividing it by the Earth surface area. This model of Earth's thermal inertia finds support in the fact that the observed Earth's energy balance since 1950 shows that almost all energy surplus is stored in the ocean (Domingues et al., 2008; Murphy et al., 2009). The mass of the body of water covering A_H is then $M_H = \rho_w A_H h$, and in the polar zone $M_L = \rho_w A_L h$, where ρ_w is the density of water. Consequently, we also have $M = M_H + M_L$, constant, where $M_H/M = x$.

By invoking the first law of thermodynamics for M_H, we obtain

$$M_H\, c\left(dT_H/dt\right) = q_{sH} - q_{H\infty} - q \tag{3}$$

where c is the specific heat of water, and q is the heat transfer rate between M_H and M_L. The radiation heat transfer model is the same as in De Vos (1992) and De Vos and Van der Wel (1993). The equatorial surface receives the solar heat current

$$q_{sH} = A_{Hp}\,(1 - \rho)\, f_H\, \sigma\, T_S^4 \tag{4}$$

where T_s, σ, f_H and ρ are the temperature of the Sun as a black body (5762 K), the Stefan Boltzmann constant ($5.67 \times 10^{-8}\,\mathrm{W\,m^{-2}\,K^{-4}}$), the Earth-Sun view factor (2.16×10^{-5}), and the albedo of the Earth ($\rho = 0.299$, in the period 2000–2004, see Trenberth et al., 2009). The area A_{Hp} is the area A_H projected on a plane perpendicular to the direction Earth-Sun. The ratio A_{Hp}/A_H decreases from $1/\pi$ when A_H is a narrow belt along the equator, to $\frac{1}{4}$ when A_H covers the globe completely:

$$A_{Hp}/A_H = f_H = \frac{\theta + \sin\theta\cos\theta}{2\,\pi\,\sin\theta} \tag{5}$$

Here θ is the latitude of the transition from A_H to A_L, with $\theta = 0$ is at the equator, and $\theta = \pi/2$ at the north pole (Fig. 1). The A_H surface radiates into space the heat current

$$q_{H\infty} = A_H\,(1 - \gamma)\,\sigma\, T_H^4 \tag{6}$$

where $\gamma \sim 0.4$ is the Earth's greenhouse factor, or the reflectance in the infrared region ($\gamma = 0.397$ in the period 2000–2004, see Trenberth et al., 2009).

The first law for the M_L portion of the crust requires

$$M_L\, c\left(dT_L/dt\right) = q_{sL} + q - q_{L\infty} \tag{7}$$

The radiative heat current received from the sun, q_{sL}, is a new feature that is added to the model of Bejan and Reis (2005):

$$q_{sL} = A_{Lp}\,(1-\rho)\,f_L\,\sigma\,T_S^4 \tag{8}$$

The radiation current transmitted to the cold background is $q_{L\infty}$,

$$q_{L\infty} = A_L\,(1-\gamma)\,\sigma\,T_L^4 \tag{9}$$

The projected area of the polar zone is related to the area of the polar zone by:

$$\left(A_{Lp}/A_L\right) = f_L = \frac{\pi/2 - \theta - \sin\theta\cos\theta}{2\,\pi\,(1-\sin\theta)} \tag{10}$$

Equations (6) and (9) have been simplified by neglecting T_∞^4 in favor of T_H^4 and T_L^4, respectively.

Finally, the heat current q is driven from T_H to T_L by the buoyancy effect in the layer of fluid that covers the Earth's surface. As shown in Bejan and Reis (2005), to derive the q formula we neglect factors of order 1, in accordance with the rules of scale analysis (Bejan, 2004). The fluid layer covers an area of flow length $L(\sim R)$ and width $W(\sim R)$. The vertical length scale of the fluid layer, H, will be defined shortly. The length L bridges the gap between T_H and T_L.

At the T_H-end of the fluid layer, the hydrostatic pressure at the bottom of the layer is $\rho_H gH$. Similarly, at the T_L-end the pressure is $\rho_L gH$. The pressure difference in the L direction is:

$$\Delta P \approx (\rho_L - \rho_H)\,gH \approx \rho\,\beta\,(T_H - T_L)\,gH \tag{11}$$

where ρ is the mean fluid density, and β is the coefficient of volumetric thermal expansion.

Discussion Paper | Discussion Paper | Discussion Paper | Discussion Paper |

ESDD

2, 241–270, 2011

Climate change, in the framework of the constructal law

M. Clausse et al.

The fluid-layer control volume is exposed to the force ΔPWH in the L direction. This force is opposed by the shear force felt by the moving fluid over the surface LW,

$$\Delta PWH = \tau LW \tag{12}$$

The average shear stress is

$$\tau \approx \rho \, \varepsilon_M \, u/H \tag{13}$$

where ε_M is the eddy diffusivity for momentum, and u is the velocity in the L direction. For the order of magnitude of ε_M we use Prandtl's mixing length model (e.g., Bejan, 2004, p. 343), in which we take H to represent the mixing length,

$$\varepsilon_M = H^2 \, u/H = Hu \tag{14}$$

In other words, H is the vertical dimension of the fluid system that mixes (transfers momentum vertically) while moving horizontally. Note that H is not the vertical extent of the fluid layer. By eliminating ΔP, u and ε_M between Eqs. (11)–(14) we obtain the horizontal velocity scale

$$u \approx \left[\beta \, g \, (T_H - T_L) \, H^2/L\right]^{1/2} \tag{15}$$

The convective heat transfer rate associated with the counterflow between T_H and T_L depends on whether the two branches of the counterflow are in intimate thermal contact. They are not if the circulation is in the plane $L \times W$, as in the case of R-scale oceanic and atmospheric currents that complete loops over large portions of the globe (Fig. 2a). Another example is when the loop is a vertical plane aligned with the meridian, when the branches of the counterflow are far enough apart and do not exchange heat in a significant way in the vertical direction (Fig. 2b). In such cases the convective heat current is

$$q \approx \rho \, u \, HW \, c_p \, (T_H - T_L) \tag{16}$$

ESDD
2, 241–270, 2011

or, after using Eq. (15) and $L \sim W \sim R$,

$$q \approx \rho \, c_p \, (g \, \beta)^{1/2} \, H^2 \, R^{1/2} \, (T_H - T_L)^{3/2} \tag{17}$$

According to constructal theory, the configuration that will prevail is the one that provides progressively greater conductance for the flow of q. It was shown in Bejan and Reis (2005) that greater access is provided by the second configuration (Fig. 2b), therefore in this paper we rely on Eq. (17) to estimate the rate of heat convection from M_H to M_L.

Note further that in writing Eqs. (3) and (7), we treated M_H and M_L as closed systems. This is permissible because the net mass flow affected by the counterflow (Fig. 2) is zero, and because the enthalpy current carried by the counterflow (q) is analogous to a heat current across a surface with zero mass flow (cf. Bejan, 2006, p. 512).

3 Numerical formulation

The dimensionless formulation of the governing equations is based on using the following scales

$$T_{scale} = f^{1/4} \, T_s = 392.8 \text{ K} \tag{18}$$

$$t_{scale} = (\rho_w \, h \, c)/(\sigma \, T^3_{scale}) \tag{19}$$

where h is the average depth of the layer of ocean water as defined in Sect. 2. The dimensionless variables are:

$$\left(\tilde{T}_H, \tilde{T}_L\right) = (T_H, T_L)/T_{scale} \tag{20}$$

$$\tilde{t} = t/t_{scale} \tag{21}$$

$$\tilde{q} = q/(\sigma \, T^4_{scale} A) \tag{22}$$

ESDD
2, 241–270, 2011

Equations (3), (7) and (17) become

$$x\left(d\,\tilde{T}_H/d\,\tilde{t}\right) = x\,f_H\,(1-\rho) - x\,(1-\gamma)\,\tilde{T}_H^4 - \tilde{q} \tag{23}$$

$$(1-x)\left(d\,\tilde{T}_L/d\,\tilde{t}\right) = (1-x)\,f_L\,(1-\rho) + \tilde{q} - (1-x)\,(1-\gamma)\,\tilde{T}_L^4 \tag{24}$$

$$\tilde{q} \approx C\left(\tilde{T}_H - \tilde{T}_L\right)^{3/2} \tag{25}$$

where C is the group

$$C = (\rho\,c_p\,(g\,\beta)^{1/2}\,H^2\,R^{1/2})/(\sigma\,A\,T_{scale}^{5/2}) \tag{26}$$

If we use $H \sim 2$ km for the thickness of the mixing layer in the atmosphere at 0 °C, $R \sim 6600$ km and $A = 4\pi R^2$, then $C \sim 0.04$. On the other hand, the conductance $C_{3/2}$ of Table 1 in Bejan and Reis (2005) corresponds to assumption that $H \sim 5.2$ km, in which case $C \sim 0.181$. The numerical results reported in the next section are based on $C = 0.181$.

In summary, there are three equations (Eqs. 23–25) containing four unknowns $\left(\tilde{T}_H, \tilde{T}_L, \tilde{q}, x\right)$, which are functions of time. The radiative parameters are assumed specified. The problem is closed by invoking the constructal law, which states that the design of the flow system evolves toward greater flow access for the heat current from the hot zone to the cold zone,

$$\partial\tilde{q}/\partial x = 0 \tag{27}$$

The evolution toward greater flow access is achieved by selecting the configuration, which is represented by x.

ESDD
2, 241–270, 2011

4 Simulation of global warming and cooling

Changes in the albedo (ρ) and the Earth's greenhouse factor (γ) are caused by many processes on the Earth's surface, including human activity. What causes these changes is not the phenomenon addressed in this paper. The problem is to determine the response of the global climate when the ρ and γ are known (e.g. measured, or predicted with confidence). The sequence of numerical simulations described next was designed to test the response of the global climate parameters $\left(\tilde{T}_H, \tilde{T}_L, x\right)$ to changes in the radiative properties of the atmosphere (ρ, γ).

To start with, as reference configuration we generated the steady state that prevails when $\rho = 0.3$ and $\gamma = 0.4$. This state is determined by solving Eqs. (20)–(22) and (24) with $d/d\,\tilde{t} = 0$ in Eqs. (20) and (21). The results are

$$\begin{aligned} \rho &= 0.3 \quad x = 0.8401 \\ \gamma &= 0.4 \quad \tilde{T}_H = 0.7471 \; (T_H = 293.5\,\mathrm{K}) \\ \tilde{T}_L &= 0.6577 \; (T_L = 258.4\,\mathrm{K}) \end{aligned} \tag{28}$$

The average surface temperature $\bar{T} = 293.5 \times 0.8401 + 258.4 \times (1 - 0.8401) = 288.3\,\mathrm{K}$ (15.2 °C) which is close to the actual value (~18 °C).

The value found for x corresponds to the latitudes 57° N and 57° S. Therefore the polar zones predicted in this paper are wider than the commonly known polar zones which correspond to the latitudes 33′44″ N and S.

4.1 Step changes in albedo and greenhouse factor

One common feature of all such simulations is that the optimal area ratio x is a function of $\tilde{t}$, ρ and γ. For the step change, x will be set at its new steady state value assuming that the area partitioning between the equatorial and the polar zones is instantaneously adapting to the new values of ρ and γ.

ESDD
2, 241–270, 2011

Climate change, in the framework of the constructal law

M. Clausse et al.

Two step changes in the albedo and the greenhouse factor are considered: (A) $\delta\rho = 0.002$ with $\delta\gamma = 0.011$, and (B) $\delta\rho = 0.002$ with $\delta\gamma = 0.005$ (Fig. 3). Four time scales are plotted: one for the non-dimensional time and three others corresponding to different ratio of ocean layer mass taken into account for Earth's inertia (case 1: 100%, case 2: 50% and case 3: 33%).

For case (A) the new steady state calculated based on the model of Sect. 3 is represented by

$$\begin{aligned} \rho &= 0.302 \quad x = 0.8398 \\ \gamma &= 0.411 \quad \Delta T_{\mathrm{H}} = 1.16\,\mathrm{K} \\ \Delta T_{\mathrm{L}} &= 1.11\,\mathrm{K} \end{aligned} \tag{29}$$

while for case (B), it is represented by

$$\begin{aligned} \rho &= 0.302 \quad x = 0.8395 \\ \gamma &= 0.405 \quad \Delta T_{\mathrm{H}} = 0.41\,\mathrm{K} \\ \Delta T_{\mathrm{L}} &= 0.41\,\mathrm{K} \end{aligned} \tag{30}$$

The overall mean temperature change is 1.15 K for case (A) and 0.41 K for case (B). The time needed for the Earth's mean temperature to reach 60% of its equilibrium response is $\tilde{t} = 0.98$ for case (A) and $\tilde{t} = 0.91$ for case (B). Depending on the mass fraction of ocean layer taken into account in the inertia calculation, these times correspond to 104, 57 and 35 years for cases 1, 2 and 3, respectively.

The evolution of the Earth's energy imbalance is also reported in Fig. 3. The energy imbalance is defined as the net heat current received from the sun ($q_{\mathrm{sH}} + q_{\mathrm{sL}}$) minus the net heat current rejected to the outer space ($q_{\mathrm{H}\infty} + q_{\mathrm{L}\infty}$):

$$q''_{\mathrm{ex}} = \left[(q_{\mathrm{sH}} + q_{\mathrm{sL}}) - (q_{\mathrm{H}\infty} + q_{\mathrm{L}\infty})\right]/A \tag{31}$$

ESDD
2, 241–270, 2011

The energy imbalance is the highest initially [3.67 W m^{-2}, case (A)], while it is still significant [1.47 W m^{-2}, case (A)] when 60% of the temperature response is reached. Although coming from a simple model, these results are consistent with those based on highly complex meteorological models. For example, using the global climate model of the NASA Goddard Institute of Space Studies to simulate the climate evolution for the 1880–2003 period, Hansen et al. (2005) have found an overall temperature increase of 1.2 K for an increase of 0.6 K after 120 years. The same authors report an energy imbalance reaching 0.85 ± 0.15 W m^{-2}for an overall energy imbalance of 1.8 W m^{-2} relative to 1880. Furthermore, 25–50 years are needed for the Earth's temperature to reach 60% of its equilibrium response. Hansen et al. (2005) also reported that 85% of the heat storage occurs above 750 m depth. The depth taken into account for thermal inertia calculation in case 3 (917 m) is of the same order of magnitude, so that only case 3 is studied in what follows.

4.2 Ramp function for ρ and γ increase

In order to improve the model, a linear increase of ρ and γ lasting 120 years is assumed. The initial and final values of ρ and γ are maintained at the same levels as those used in Sect. 4.1. The x value is optimised at every time step during the evolution of ρ and γ.

The temperature and energy imbalance evolutions are presented on Fig. 4 by assuming that the Earth's inertia is equal to one third of the ocean mass (cf. case 3 in Sect. 4.1).

The steady states are the same as those reported in Sect. 4.1, Eqs. (29) and (30). At $t = 120$ years and for a γ increase of 0.011, the temperature increase is 0.7 K for polar zone while it reaches 0.81 K for the equatorial zones. Comparing with results found by Hansen et al. (2005), our calculated values are in relatively good agreement with those found by these authors: 0.77 K for the mean temperature increase, and 1.1 W m^{-2} for the energy imbalance in our case compared to 0.6 K and 0.85 W m^{-2}, respectively for about the same period of time.

As the values of γ and ρ were kept constant after 120 years, the results obtained after that date could be compared to those found by Wigley (2005) for his constant concentration (CC) scenario. In his case, the reference year is year 2000, which in our case corresponds to an elapsed time of 120 years.

If we compare the results at year 2200 (i.e., an elapsed time of 320 years in our case), our calculations match quite well Wigley'results for the case of the CC scenario: case (A) is close to his central climate sensitivity scenario (0.36 K compared to 0.33 K, respectively) while case (B) is close to the low sensitivity scenario (0.13 K compared to 0.15 K).

4.3 Continuous increases in ρ and γ

In this section, we present the results for a continuous linear increase of γ and ρ. The rates are equal to those used in Sect. 4.2, case (A). This model gives an idea of the Earth's response to a "business as usual" scenario. Two scenarios are considered:

- Case (A), the rates of increase for γ and ρ are equal to their respective values used in Sect. 4.2: $\gamma = 0.4 + \frac{0.011 \cdot \tilde{t}}{3.45}$ and $\rho = 0.3 + \frac{0.002 \cdot \tilde{t}}{3.45}$.

This represents an optimistic view for γ, as it is known that the CO_2 emission rate has greatly increased in the past 50 years. Hence, the IEA (2008) reports global emissions equal to 20 945 M tons yr^{-1} of CO_2 in 1990, 27 889 M tons y^{-1} in 2006 but 40 553 M tons y^{-1} are foreseen in 2030. To improve our model, a change in the rate for γ (doubling), starting at year 2000, is implemented and corresponds to case (B):

- Case (B) is identical to case (A) for $\tilde{t} \leq 3.45$ (~120 years), and above this value the γ increase rate is multiplied by a factor of two: $\gamma = 0.4 + \frac{0.022 \cdot (\tilde{t} - 3.45)}{3.45}$ and $\rho = 0.3 + \frac{0.002 \cdot \tilde{t}}{3.45}$ for $\tilde{t} > 3.45$.

The origin of time still corresponds to the year 1880, as it was the case in Sect. 4.2. Figure 5 shows that after 320 years the mean temperature increase is roughly 2.5 K for case (A) and 4.3 K for case (B). For the period between 120 and 320 years, this corresponds to an increase of 1.88 K and 3.75 K for cases (A) and (B), respectively. Comparing these last results with the values found by Wigley (2005) in his constant emissions (CE) scenario at year 2200, case (B) is slighlty above the Wigley's value for high climate sensitivity to CO_2 doubling (3.3 K) while case (A) is almost equal to the value found by Wigley for medium climate sensitivity (2.1 K).

Another reading of Fig. 5, is to evaluate the remaining time before reaching a temperature increase of 2 K, value above which, the consequences on climate are seen to be irreversible. This threshold is reached after 200 and 250 years for cases (A) and (B), respectively. Hence, measured from today, there remain 70 years in the worst case before reaching the 2 K increase. Lowering the CO_2 emissions to a rate close to that between years 1880 and 2000, would result in a 50 years delay only.

Concerning the energy imbalance, it is evaluated by Wigley (2005) at 3.7 W m^{-2} for a CO_2 doubling. The values found based on our model 1.2 W m^{-2} and 2.7 W m^{-2} remain below those of Wigley. However, the comparison between these values is not straightforward, as Wigley's value is achieved for CO_2 concentration doubling whereas in our case the energy imbalance depends on ρ and γ evolutions.

5 Continuous earth temperature model

In this section we examine more closely the heat flow in the poleward direction, and how this flow depends on the albedo (ρ) and the Earth's greenhouse factor (γ). Consider an infinitesimal ring of radius $R\cos\theta$ The width of the Earth' surface at the latitude θ is $Rd\theta$. The area perpendicular to the sunrays is $2R^2\cos^2\theta d\theta$ (see Fig. 6). The heat balance in such a ring requires:

$$2R^2 f (1-\rho)\sigma T_s^4 \cos^2\theta\, d\theta - 2\pi R^2 (1-\gamma)\sigma T^4 \cos\theta\, d\theta - dq = 0 \qquad (32)$$

ESDD
2, 241–270, 2011

where all the symbols have the same significance as in the preceding sections. The excess heat current q in the ring is convected toward the poles (the cold sinks) by the Earth's global circulation. Therefore the variation of the poleward heat flow with latitude is given by:

$$dq/d\theta = 2R^2\sigma\cos\theta\left[f(1-\rho)T_s^4\cos\theta - \pi(1-\gamma)T^4\right] \tag{33}$$

The heat flow at the latitude θ is obtained by integrating Eq. (33) from 0 to θ:

$$q(\theta) = \int_0^\theta 2R^2\sigma\left[f(1-\rho)T_s^4\cos^2\theta - \pi(1-\gamma)T^4\cos\theta\right]d\theta \tag{34}$$

By using the mean value of T^4 it is possible to estimate the hemispheric poleward heat current as:

$$q(\theta) \approx 2R^2\sigma\left[f/2(1-\rho)T_s^4\left(\sin(2\theta)/2+\theta\right) - \pi(1-\gamma)\bar{T}^4\sin\theta\right] \tag{35}$$

Because $q(\theta)$ must be zero at the pole, Eq. (35) offers the opportunity to evaluate the average surface temperature $\bar{T}$. Therefore, with $\theta=\pi/2$, and assuming $\bar{T}^4 \sim (\bar{T})^4$ (note that the error involved here is of order $12\sigma_T^2/(\bar{T})^2 \sim 0.06$, where σ_T is the standard error), Eq. (35) yields

$$\bar{T} \sim \left[f(1-\rho)/4(1-\gamma)\right]^{1/4} T_s \tag{36}$$

Additionally, symmetry requires $dq/d\theta=0$ at the equator. Therefore, we obtain the equator temperature from Eq. (32) as :

$$T_{eq} = \left[f(1-\rho)/\pi(1-\gamma)\right]^{1/4} T_s \tag{37}$$

By using $\rho=0.3$ and $\gamma=0.4$, we obtain $\bar{T}\sim 288.7$ K (15.5 °C), which is close to the actual value (~18 °C), and $T_{eq}=306.7$ K (33.5 °C), which is also close to the observed value. A rough estimate of the pole temperature is $T_p \approx 2\bar{T} - T_{eq} = 270.7$ K (−3.1 °C), which corresponds to a temperature difference of 36 K between equator and pole.

ESDD

2, 241–270, 2011

Both $q(\theta)$ and $dq/d\theta$ are presented in Fig. 7. We see that q has a maximum close to the latitude 35°, and it drops to zero at the equator and the poles. In the representation of $dq/d\theta$, a linear estimate of the local temperature $T(\theta) \approx T_{eq} - 2\theta/\pi \cdot (T_{eq} - T_p)$ has been used. We observe that between the equator and the latitude 35° the Earth's surface contributes positively to the poleward heat flow, while from latitude 35° onwards the Earth's surface absorbs heat from that flow.

The current increase in aerosol concentration in the atmosphere leads to an increase in the cloud cover (Givati and Rosenfeld, 2004) which combined with the direct effect of light reflection by aerosols increases the albedo ρ of the earth. As a consequence, less solar radiation is absorbed at the surface. On the other hand, the increasing concentration of greenhouse gases has the effect of impeding the escape of terrestrial radiation into space, thus increasing the greenhouse factor γ. The trade-off between these opposing trends results in a net positive radiative imbalance of order $q''_{ex} = 0.85\,\mathrm{W\,m^2}$ (Hansen et al., 2005).

The sensitivity of the average surface temperature to changes in ρ and γ can be calculated from Eq. (36), and is plotted in Fig. 8 for both cases in which ρ and γ have the same and opposite sign of variation. We see that the effect on temperature is higher when ρ and γ vary in opposite directions. The actual trend must correspond to a curve between these two extremes, and must stay close to the curve $d\rho = d\gamma$.

By invoking the constructal law we can anticipate the effect of these trends the Earth temperature along the meridian. At every latitude θ the heat flow (Eq. 34) depends on the albedo ρ, greenhouse factor γ (which are constrained) and temperature T (which is the free parameter). The constructal law requires maximum heat flow at all latitudes, therefore by maximizing $q(\theta)$ of Eq. (34) we obtain

$$\delta T = \left[\bar{T}/(1-\gamma)\right] \left[-(f \cos\theta/4\pi)\left(T_s/T\right)^4 \delta\rho + (1/4)\,\delta\gamma\right] \tag{38}$$

The latitudinal temperature variation for various cases is shown in Fig. 9. Here we used the average temperature based on Eq. (35). The variations $\delta\rho \sim 0 - 0.002$ and $\delta\gamma \sim 0.005$ generate positive temperature changes of order 0.6 K, which match the

ESDD
2, 241–270, 2011

observed value corresponding the past 100 years (IPCC Synthesis Report, 2007).

Except for the cases in which the albedo maintains its current value, the changes in the surface temperature vary with latitude and show higher temperature increase in the polar regions. This effect reduces the equator-to-pole temperature difference therefore reducing the poleward heat flow (Eq. 17). This reduction is shown in Fig. 10 for the case in which $\delta\rho = 0.002$ and $\delta\gamma = 0.005$ and amounts to –2.7% (see Figs. 7 and 10). Furthermore, the larger temperature increase in the polar regions (~0.2 °C) is consistent with the actual reduction in iced areas around the poles. Note also that the reduction in the solar radiation absorbed at the surface is of order $\delta\rho/(1-\rho) \sim 0.3\%$ (Eq. 4).

The poleward heat flow calculated with Eq. (34) (and Fig. 7) at the latitudes 25° and 53° that represent the boundaries between the Hadley and Ferrel cells and the Ferrel and polar cells, has practically the same values as those resulting from the constructal configuration of the global circulation (Bejan and Reis, 2006). The heat flow values calculated based on Eq. (34) are $q_{25^\circ} \sim 5.5 \times 10^{15}$ W and $q_{53^\circ} \sim 6 \times 10^{15}$ W, while those presented in Bejan and Reis (2006) are $q_{25^\circ} \sim 4.5 \times 10^{15}$ W and $q_{53^\circ} \sim 6.2 \times 10^{15}$ W, respectively.

6 Conclusions

Complex models of the Earth thermal behaviour are opaque from the point of view of the general audience, and contain the uncertainties of the many flows of various scales that are included in these models. On this background, simple models provide interesting results even if with fewer details. In this paper, a simple convection/radiation model was used for anticipating the time-dependent response of the Earth climate to changes in the albedo and greenhouse factor. The novelty is the simplicity, transparency and the use of constructal law as the principle that governs the evolution of flow configuration in time, and which provides closure of the model equations.

In the first part of the paper the model was tested for the actual state of the Earth, by using the measured values of the Earth's albedo and greenhouse factor. The results were consistent with the actual thermal state of the Earth and the equator to pole temperature difference. The thermal response of the Earth was then tested for changes in the Earth's albedo and greenhouse factor, namely ($\delta\rho = 0.002$; $\delta\gamma = 0.011$) and ($\delta\rho = 0.002$; $\delta\gamma = 0.005$). The results indicated that equatorial and polar temperatures increase by ($\Delta T_H = 1.16$ K; $\Delta T_L = 1.11$ K) and ($\Delta T_H = 0.41$ K; $\Delta T_L = 0.41$ K), respectively. The time needed for the Earth mean temperature to reach 60% of its equilibrium response is 104 and 57 years, respectively, while the radiative imbalance is of the same order as the measured value ($0.85 \pm 0.15\,\mathrm{W\,m^{-2}}$).

In the second part of the paper we used a continuous model of changing atmospheric radiative properties. These values determined for the equator and polar temperatures and the equatorial to pole temperature difference that are consistent with the actual values. A continuous mapping of Earth forcing through changes in albedo and greenhouse factor was obtained for the domain between $\delta\rho = \delta\gamma$ and $\delta\rho = -\delta\gamma$. It was shown that the values of the actual global warming are consistent with forcing amplitudes close to $\delta\rho = 0.002$ and $\delta\gamma = 0.005$. An additional result is that the poleward heat current reaches its maximum close to the latitude 35°, therefore indicating that between this latitude and the pole the Earth thermal budget is negative. This latitude corresponds to the position of the Ferrel cell in the global circulation, which is driven by the Hadley cell that exports heat and the Polar cell, which acts as heat receiver.

Acknowledgements. A. H. Reis' work was supported by Fundação para a Ciência e Tecnologia (Portugal) under the project PTDC/EME-MFE/71960/2006. Adrian Bejan's contribution was supported by grants from the US National Renewable Energy Laboratory (Golden, Colorado) and the US Air Force Office of Scientific Research.

ESDD
2, 241–270, 2011

Climate change, in the framework of the constructal law

M. Clausse et al.

References

Bejan, A.: Advanced Engineering Thermodynamics, 2nd editon, Wiley, New York, ch. 13, 1997.
Bejan, A.: Shape and Structure, from Engineering to Nature, Cambridge University Press, Cambridge, UK, 2000.
Bejan, A.: Convection Heat Transfer, 3rd edition, Hoboken, 2004.
Bejan, A: Advanced Engineering Thermodynamics, 3rd edition, Wiley, Hoboken, 2006.
Bejan, A. and Reis, A. H.: Thermodynamic optimization of global circulation and climate, Int. J. Energ. Res., 29, 303–316, 2005.
Bejan, A. and Lorente, S.: Constructal theory of generation of configuration in nature and engineering, J. Appl. Phys., 100, 1–27, 2006.
De Vos, A.: Endoreversible Thermodynamics of Solar Energy Conversion, Oxford University Press, Oxford, UK, 53–67, 1992.
De Vos, A. and Van der Wel, P.: The efficiency of the conversion of solar energy into wind energy by means of Hadley cells, Theor. Appl. Climatol., 46, 193–202, 1993.
Domingues, C. M., Church, J. A., White, N. J., Gleckler, P. J., Wijffels, S. E., Barker, P. M., and Dunn, J. E.: Improved estimates of upper-ocean warming and multi-decadal sea-level rise, Nature, 453, 1090–1093, 2008.
Givati, A. and Rosenfeld, D.: Quantifying precipitation suppression due to air pollution, J. Appl. Meteorol., 43, 1038–1056, 2004.
Hansen, J., Nazarenko, L., Ruedy, R., Sato, M., Willis, J., Del Genio, A., Koch, D., Lacis, A., Lo, K., Menon, S., Novakov, T., Perlwitz, J., Russell, G., Schmidt, G. A., and Tausnev, N.:, Earth's Energy Imbalance: Confirmation and Implications, Science, 308(3), 1431–1434, 2005.
IEAWorld Energy Outlook: International Energy Agency report, 2008.
IPCC Synthesis Report: http://www.ipcc.ch/pdf/assessment-report/syr/ar4_syr.pdf (last access: March 2011), 2007.
Lin, C. A.: An extremal principle for a one-dimensional climate model, Geophys. Res. Lett., 9, 716–718, 1982.
Lorenz, E. N.: Available potential energy and the maintenance of the general circulation, Tellus, 7, 157–167, 1955.
Lorenz, R. D., Lunine, J. I., McKay, C. P., and Withers P. G.: Titan, Mars and Earth: entropy production by latitudinal heat transport, Geophys. Res. Lett., 25, 415–418, 2001.

ESDD
2, 241–270, 2011

Climate change, in the framework of the constructal law

M. Clausse et al.

Malkus, W. V. R.: The heat transport and spectrum of turbulence, P. Roy. Soc. Ser. A, 225, 196–212, 1954.
Murphy, D. M., Solomon, S., Portmann, R. W., Rosenlof, K. H., Forster, P. M., and Wong, T.: An observationally based energy balance for the Earth since 1950, J. Geophys. Res., 114, D17107, doi:10.1029/2009JD012105, 2009.
North, G. R.: Energy balance climate models, Rev. Geophys. Space Ge., 19, 91–121, 1981.
Paltridge, G. W.: Global dynamics and climate – a system of minimum entropy exchange, Q. J. Roy. Meteor. Soc., 101, 475–484, 1975.
Paltridge, G. W.: The steady-state format of global climate, Q. J. Roy. Meteor. Soc., 104, 927–945, 1978.
Reis, A. H.: Constructal theory: from engineering to physics and how flow systems develop shape and structure, Appl. Mech. Rev., 59, 269–282, 2006.
Reis, A. H. and Bejan, A.: Constructal theory of global circulation and climate, Int. J. Heat Mass Tran., 49, 1857–1875, 2006.
Schulman, L. L.: A theoretical study of the efficiency of the general circulation, J. Atmos. Sci., 34, 559–580, 1977.
Swenson, R.: Emergent attractors and a law of maximum entropy production: foundations to a theory of general evolution, Syst. Res., 6, 187–197, 1989.
Trenberth, K. E., Fasullo, J. T., and Kiehl, J: Earth's global energy budget, B. Am. Meteorol. Soc., 311–323, 2009.
Whitfield, J.: Order out of chaos, Nature, 436(7053), 905–907, 2006.
Wigley, T. M. L.: The Climate Change Commitment, Science, 307, 1766–1769, 2005.

ESDD
2, 241–270, 2011

Climate change, in the framework of the constructal law

M. Clausse et al.

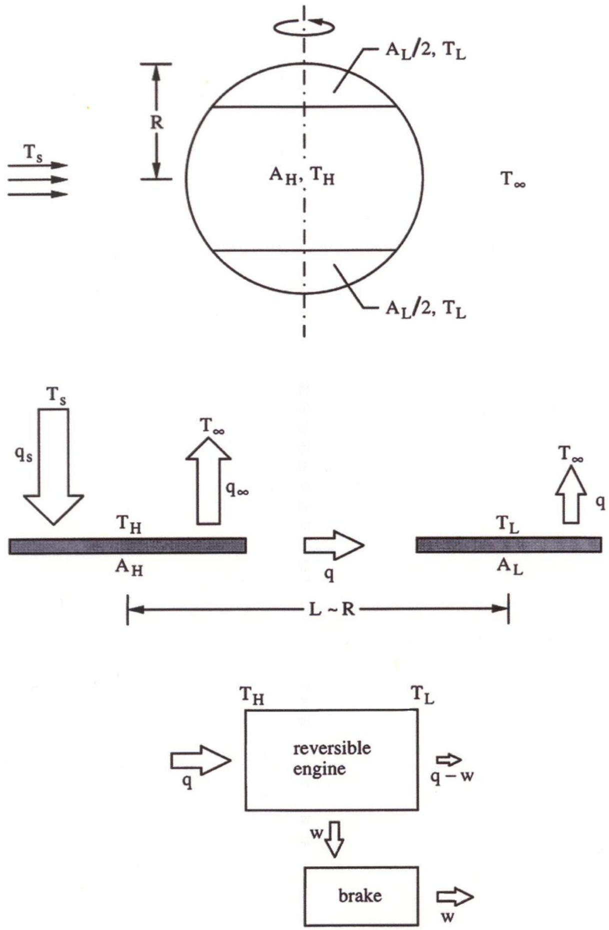

Fig. 1. Earth model with warm (A_H) and cold (A_L) zones, latitudinal convective heat current between them.

ESDD
2, 241–270, 2011

Climate change, in the framework of the constructal law

M. Clausse et al.

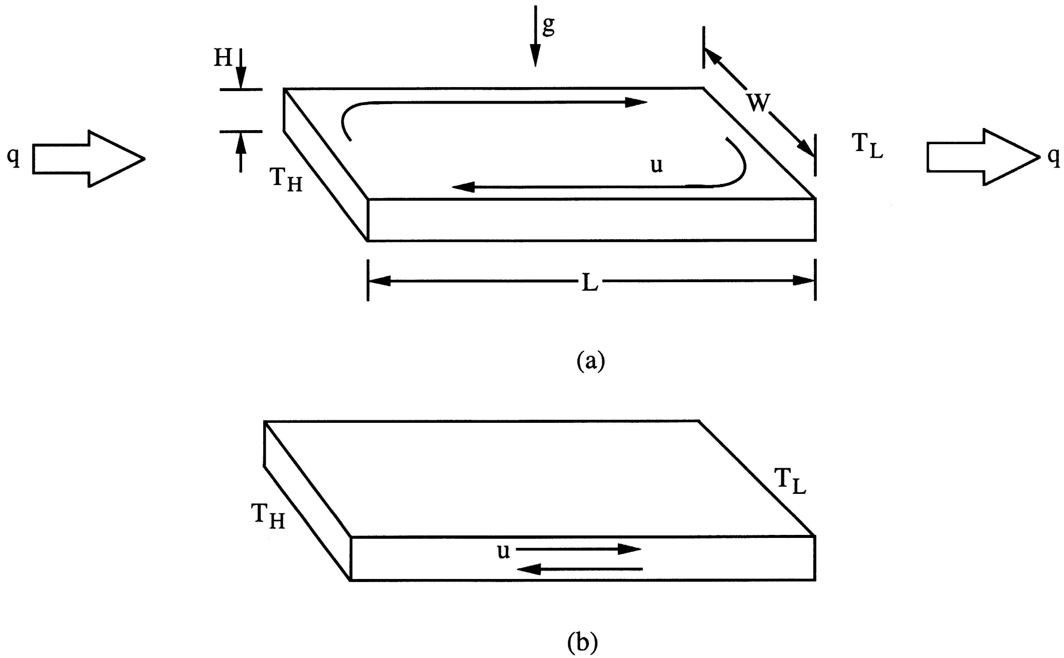

Fig. 2. Convection loops in the fluid layer connecting the warm and cold zones.

ESDD
2, 241–270, 2011

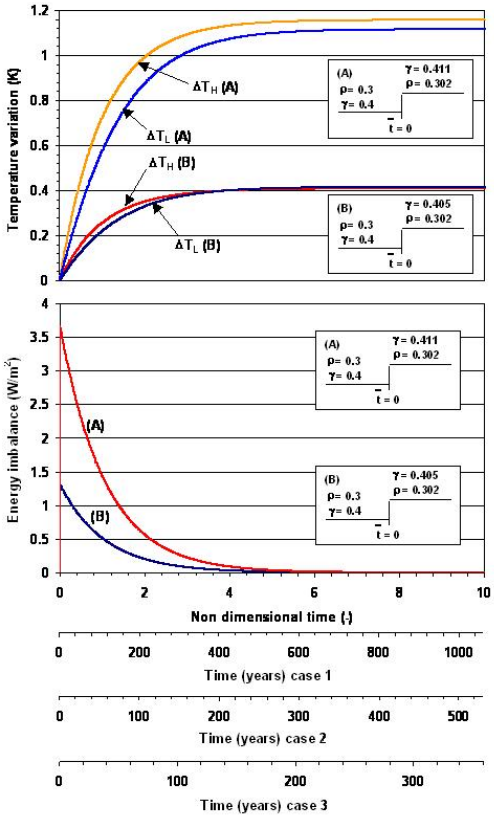

Fig. 3. Earth's energy flux imbalance and temperature increase for the polar zone (ΔT_L) and the equatorial zone (ΔT_H) evolutions in response to two different step changes in albedo (ρ) and greenhouse factor (γ). Four time scales are plotted: non dimensional time, and three cases corresponding to different ratio of ocean layer mass taken into account for Earth's inertia (case 1: 100%, case 2: 50% and case 3: 33%).

ESDD
2, 241–270, 2011

Climate change, in the framework of the constructal law

M. Clausse et al.

Title Page
Abstract Introduction
Conclusions References
Tables Figures
◂ ▸
Back Close
Full Screen / Esc
Printer-friendly Version
Interactive Discussion

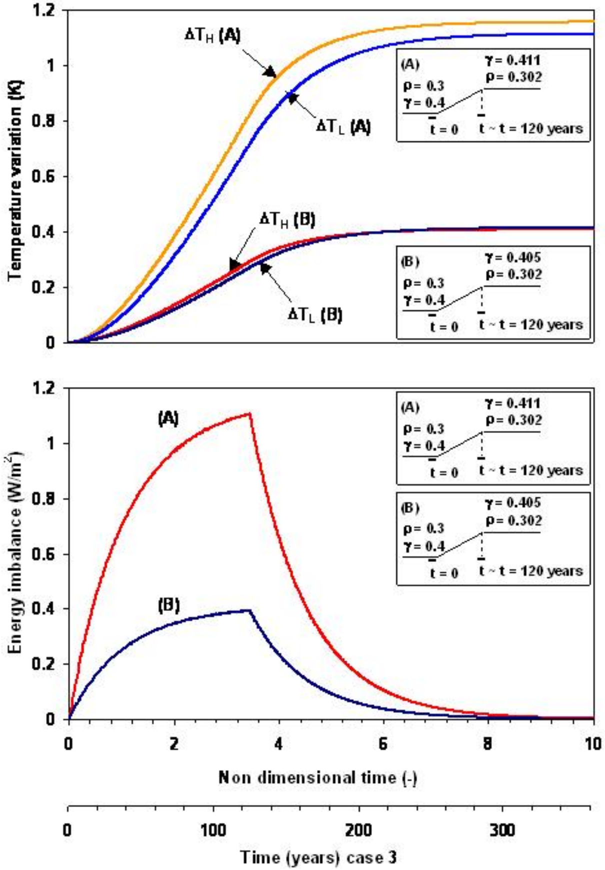

Fig. 4. Earth's energy flux imbalance and temperature increase for the polar zone (ΔT_L) and the equatorial zone (ΔT_H) evolutions in response to two different ramp changes in albedo (ρ) and greenhouse factor (γ).

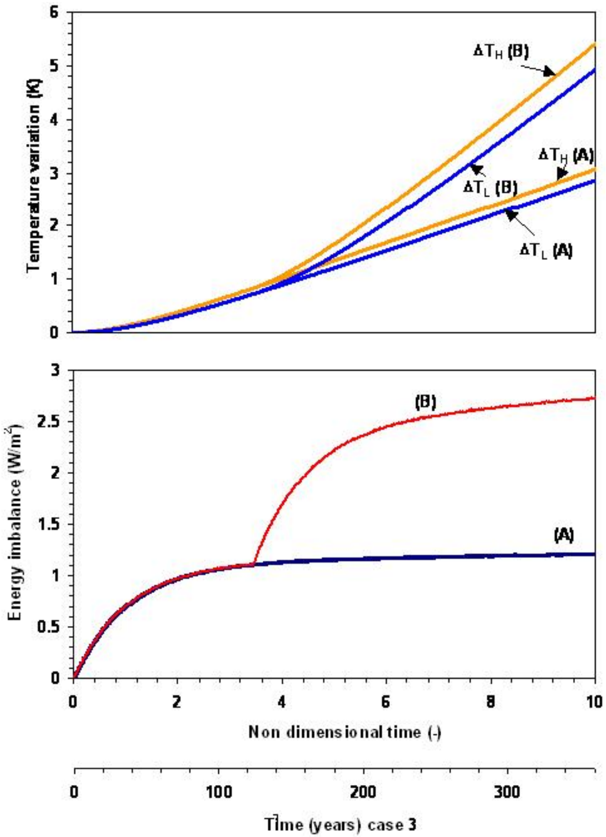

Fig. 5. Earth's energy flux imbalance and temperature increase for the polar zone (ΔT_L) and the equatorial zone (ΔT_H) evolutions in response to a continuous change (constant emission scenario) in albedo (ρ) and greenhouse factor (γ). Case (A): $\gamma = 0.4 + \frac{0.011 \cdot \tilde{t}}{3.45}$ and $\rho = 0.3 + \frac{0.002 \cdot \tilde{t}}{3.45}$. Case (B) same as case (A) for $\tilde{t} \le 3.45$ (~120 years); $\gamma = 0.4 + \frac{0.022 \cdot (\tilde{t} - 3.45)}{3.45}$ and $\rho = 0.3 + \frac{0.002 \cdot \tilde{t}}{3.45}$ for $\tilde{t} > 3.45$.

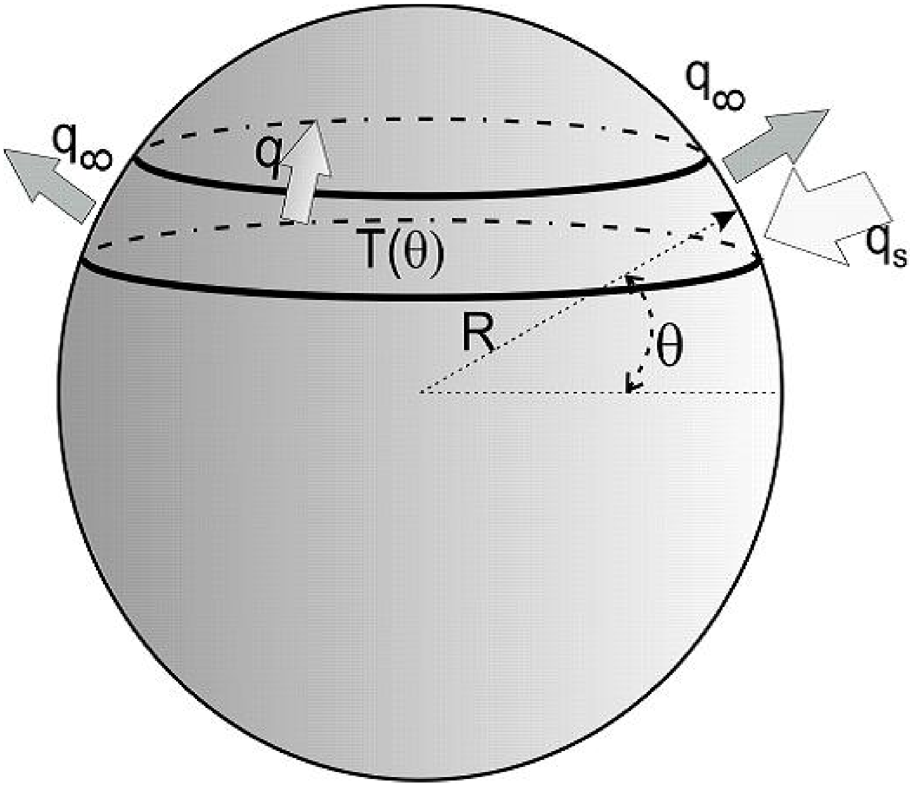

Fig. 6. Heat flows in a control surface ring at latitude θ: q_s represents the solar radiation absorbed at the surface, q_∞ is terrestrial radiation emitted into the outer space, and q is the imbalanced heat flow convected over the earth's surface.

ESDD
2, 241–270, 2011

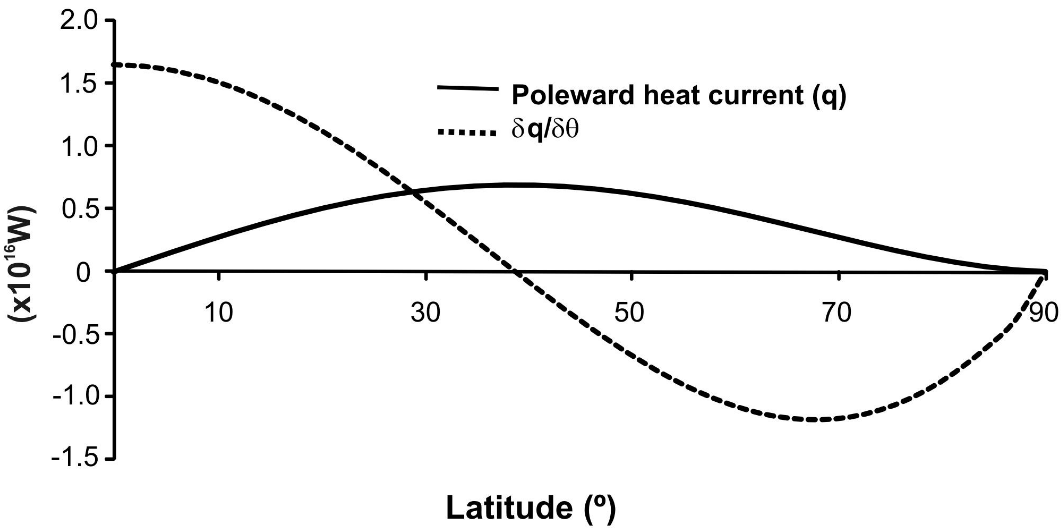

Fig. 7. Poleward heat flow and its variation with latitude. Note that from the equator onto the latitude 35° heat is continuously added to the heat flow q, while heat is removed from q between latitude 35° and the pole.

ESDD
2, 241–270, 2011

Climate change, in the framework of the constructal law

M. Clausse et al.

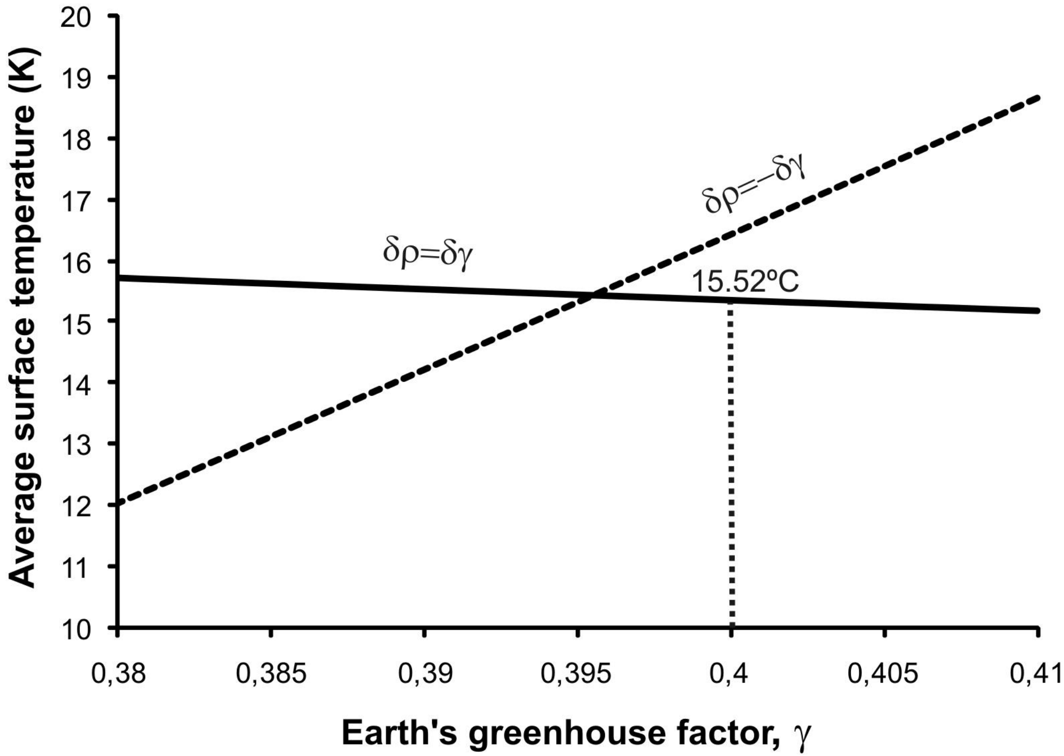

Fig. 8. Average surface temperature as function of the earth's greenhouse factor for variations of the albedo with the same and opposite sign of the variations of the earth's greenhouse factor.

ESDD
2, 241–270, 2011

Climate change, in the framework of the constructal law

M. Clausse et al.

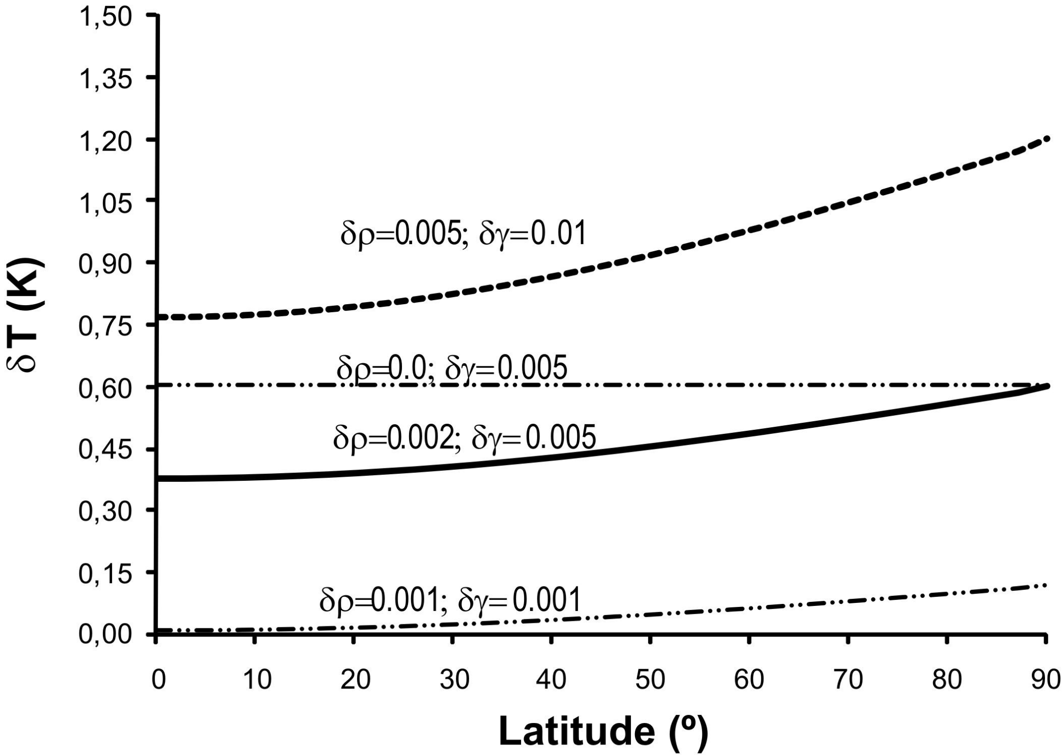

Fig. 9. Changes of the surface temperature with latitude for various changes in the albedo and the earth's greenhouse factor. The variations $\delta\rho = 0$–0.002 and $\delta\gamma = 0.005$ generate changes in surface temperature of order 0.6 °C that is the observed value. Latitudinal changes are due to changes in the albedo solely.

ESDD
2, 241–270, 2011

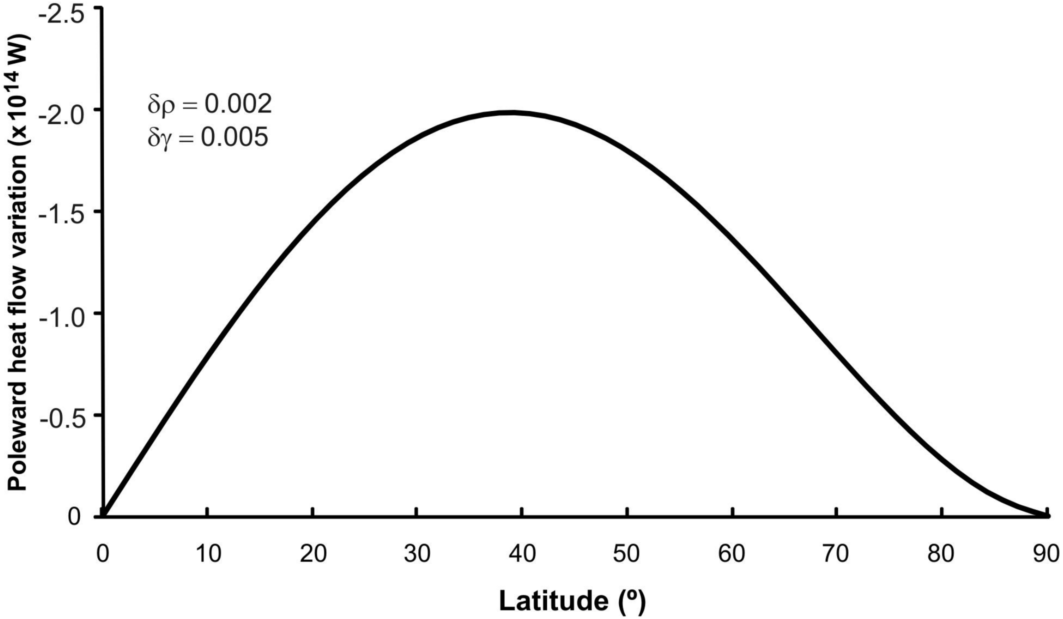

Fig. 10. Reduction of the poleward heat flow as function of latitude due to increase in the albedo and the earth's greenhouse factor ($\delta\rho = 0.002$ and $\delta\gamma = 0.005$).

ESDD
2, 241–270, 2011

Climate change, in the framework of the constructal law

M. Clausse et al.